Genetic variation of heat tolerance in a model ectotherm: an approach using thermal death time curves

Félix P. Leiva[1,2,*], Mauro Santos[3,4], Edwin J. Niklitschek[5,6], Enrico L. Rezende[7] and Wilco C.E.P. Verberk[2]

[1]Alfred Wegener Institute, Helmholtz Centre for Polar and Marine Research, 27570 Bremerhaven, Germany

[2]Department of Ecology, Radboud Institute for Biological and Environmental Sciences, Radboud University Nijmegen, 6500 GL Nijmegen, The Netherlands

[3]Departament de Genètica i de Microbiologia, Grup de Genòmica, Bioinformàtica i Biologia Evolutiva (GBBE), Universitat Autonòma de Barcelona, Bellaterra, Barcelona 08193, Spain

[4]Institute of Evolution, Centre for Ecological Research, Konkoly-Thege Miklós út 29-33, H-1121, Budapest, Hungary

[5]Centro i~mar, Universidad de Los Lagos, Km 6, Camino a Chinquihue, Casilla 557, Puerto Montt 5480000, Chile

[6]Universidad Austral de Chile, Programa de Investigación Pesquera UACH-ULAGOS, Los Pinos S/N, Puerto Montt 5480000, Chile

[7]Center of Applied Ecology and Sustainability (CAPES), Facultad de Ciencias Biológicas, Pontificia Universidad Católica de Chile, Santiago 6513677, Chile

*Corresponding author e-mail: felixpleiva@gmail.com

Word counts: 3,341 words

Abstract

The assessment of thermal tolerance holds significant importance in predicting the physiological responses of ectotherms, particularly in elucidating their capacity for evolutionary adaptation in the context of global warming. Current approaches to assessing thermal tolerance have limitations that can lead to misleading results, especially with regard to the heritability of thermal limits. In this study, we examined twenty isogenic lines of *Drosophila melanogaster* from the DGRP panel to characterize their thermal death time (TDT) curves, which account for the duration and intensity of heat stress. Furthermore, we examined the extent of genetic variation in the intercept and slope of the linear TDT curves, which are labelled as CTmax and thermal sensitivity *z*. Our analysis revealed evidence of heritable variation in each of the two parameters. Furthermore, simulations of the evolutionary consequences of selection on either CTmax or *z* indicate that selection on one parameter induces changes in the other parameter as a correlated response. We conclude that the evolution of thermosensitive or thermotolerant strategies is better achieved by directional selection to decrease or increase CTmax, which may aid in mitigating the effects of global warming on ectotherms.

Keywords: global warming, heritability, isogenic lines, thermal death time curves

1. Introduction

There is substantial evidence pointing to an unprecedented rise in the temperature of our planet. According to climate models, if the present warming trends persist, the surface temperature of the Earth's surface will surpass the average at the end of the 19th century by 1.5ºC [1]. It is not surprising that this rise will have repercussions on the biota present on our planet, particularly for animals such as ectotherms, whose physiological processes are closely linked to ambient temperature [2,3]. Climate change is already having an impact at the demographic level. Many species are shifting their ranges, often towards cooler regions [4], while others are threatened with extinction [5]. In contrast, some lineages are already able to withstand high temperatures [6], while others show phenotypic plasticity [7], and some species may evolve in response to warming [8,9]. Assessing the adaptive capacity and heritability of heat tolerance is challenging, as inaccuracies in models can lead to either under- or overestimation of vulnerability to climate change [10,11].

The current debate about the evolutionary potential of heat tolerance in ectotherms can be summarized in two main points. First, there is the notion that ectotherms exhibit limited variation in heat tolerance, suggesting that heat tolerance is evolutionary constrained. Natural selection appears to affect physiological responses to lower temperatures more than to higher temperatures [12]. Interspecific studies have generally failed to detect genetic variability in heat tolerance, variation between species and populations, and a lack of latitudinal diversity [13,14]. Likewise, selection and heritability experiments on single species suggest limited increases in upper thermal limits. Second, a complicating factor in understanding the genetic basis of upper thermal limits is that these are to some extent affected by methodological issues [for a review, see 12]. In dynamic assays, heat tolerance is typically evaluated by determining the upper critical thermal maximum (CTmax). This is measured as the temperature at which an ectotherm loses motor function when exposed to gradually increasing temperatures. The CTmax represents the highest ambient temperature an ectotherm can withstand under specific experimental conditions before succumbing to heat stress [15,16]. Studies using this dynamic assays have found suggest a limited evolutionary potential for ectotherms to increase their ability to tolerate high temperatures [17]. Despite the possibility of methodological issues underestimating the actual evolutionary potential to withstand increasing temperatures [10], it is imperative to acknowledge that a critical thermal limit is merely a component of the more intricate trait "thermal tolerance" [18].

To circumvent this limitation, an increasing number of studies have employed thermal death time (TDT) curves to measure heat tolerance [19–24]. TDT curves [sensu 25], acknowledges that survival probability is influenced by both temperature and exposure time [26,27], and may provide a more nuanced view of the two reasons mentioned above for the ongoing debate. However, the extent to which TDT curves reflect evolutionary changes within a species remains unclear. In this context, we take advantage of recent research using the Drosophila Genetic Reference Panel (DGRP) [18,28] to investigate the genetic variation of heat tolerance in *Drosophila melanogaster* using TDT curves. The wild-type DGRP lines of this panel are derived from a single natural population and have been inbred to homozygosity, providing extensive information on genetic variation at multiple levels [29] and offering unique opportunities to quantify the genetic basis of physiological traits such as heat tolerance.

2. Material and methods

(a) Experimental flies and rearing conditions

Twenty inbred, isogenic wild-type *Drosophila melanogaster* (Meigen 1830) lines from the Drosophila Genetic Reference Panel (DGRP) were used as the study model. These lines were previously employed in a study with a different objective [21], and we assume that this subset represents an approximately random collection with respect to the focus of interest described here.

All twenty selected lines were obtained from the Bloomington Drosophila Stock Center in March 2018. They were maintained in quarantine on standard cornmeal-agar-yeast media at room temperature (approximately 22°C) for four generations until May 2018. The rearing conditions were identical to those detailed in Leiva et al. [21].

(b) Thermal death time (TDT) curves

We measured the heat tolerance of individual female and male flies using a similar experimental protocol as outlined in Verspagen et al. [24]. This involved using a heating circulating bath and a wireless thermometer to measure temperature consistently throughout each trial. Individual virgin flies were placed in sealed 4-mL glass vials, arranged on a Plexiglas™ rack, and submerged in a 9.5-L glass aquarium filled with water set to a constant temperature of 36, 37, 38, or 39°C. During each trial, a Nikon D5300 with the time-lapse feature captured images at 10-second intervals. Subsequently, the compiled images were transformed into reversed videos using the open-source software Blender. Before initiating the thermal tolerance experiments, the flies were allowed approximately 30 minutes in the vials at room temperature for recovery following light CO_2 anaesthesia. This recovery period proved effective, as the flies exhibited active flying or walking inside the vial.

A total of 1,686 flies underwent survival time measurements, and the parameters of the thermal death time (TDT) curves CTmax and *z* were calculated for each DGRP line and sex. The calculation utilized the equation outlined in Rezende et al. [26]:

$$log_{10}\, t = \beta_0 + \beta_1 T = \frac{\mathrm{CTmax} - T}{z} \quad (1)$$

where *t* represents the survival time in minutes, CTmax is the temperature (°C) where the survival time is $\log_{10} t = 0$ after 1 min of exposure to assay temperature, *T* is the assay temperature (°C), and the thermal sensitivity *z* is the temperature change (°C) required for a ten-fold difference in survival time. We controlled assay temperature *T* and measured time as the dependent variable. The estimation of CTmax and *z* for each DGRP line and sex involved regression analysis of $\log_{10}$-transformed survival times against the four temperature treatments and a back-transformation where CTmax = β_0/β_1 and z = $1/\beta_1$.

(c) Estimation of variance components and broad-sense heritability of CTmax and *z*

For each DGRP genotype, we first assessed the effect of stressful temperatures (covariate) on survival time $(\mathrm{in}\ log_{10} min)$ by using for each sex the following general mixed ANCOVA model that allows separating slopes and intercepts:

$$Survival\ time\ =\ \beta_0 +\ \beta_1 \cdot stress\ T^a +\ \mu_0 Z +\ \mu_1 Z \cdot stress\ T^a + \varepsilon \quad (2)$$

where

β_0 and β_1: intercept and slope of the fixed effect of stress temperature $stress T^a$,

μ_0: vector of random coefficients representing the effect of each genotype on β_0,

μ_1: vector of random coefficients representing the effect of each genotype on β_1,

Z: Design matrix (array of dummy variables) representing the genotypes,

ε: vector of random errors

We fitted linear mixed-effects models [30] and obtained various estimates of the variance components $\hat{\sigma}^2_{\hat{\beta}_{0i}}$ $(i = 1, \cdots, 20)$, $\hat{\sigma}^2_{\hat{\beta}_{1i}}$ and $\hat{\sigma}^2_{\varepsilon}$ (caret denotes "estimate") that refer, respectively, to the variation in the intercepts and slopes of the TDT curves for the DGRP genotypes, and the residual variation. Model coefficients and variance components were then used to estimate $\mathrm{CTmax}_i = \frac{-\hat{\beta}_{0i}}{\hat{\beta}_{1i}}$ and $z_i = \frac{-1}{\hat{\beta}_{1i}}$, whose Taylor expanded variances [31, p. 240], became,

$$\mathrm{Var}\left(\mathrm{CT}_{\max_i}\right) = \mathrm{Var}\left(\frac{-\hat{\beta}_{0i}}{\hat{\beta}_{1i}}\right) \approx \frac{\left(\mu_{-\hat{\beta}_{0i}}\right)^2}{\left(\mu_{\hat{\beta}_{1i}}\right)^2}\left[\frac{\hat{\sigma}^2_{-\hat{\beta}_{0i}}}{\left(\mu_{-\hat{\beta}_{0i}}\right)^2} + \frac{\hat{\sigma}^2_{\hat{\beta}_{1i}}}{\left(\mu_{\hat{\beta}_{1i}}\right)^2} - 2\frac{\mathrm{Cov}(-\hat{\beta}_{0i}, \hat{\beta}_{1i})}{\mu_{-\hat{\beta}_{0i}}\mu_{\hat{\beta}_{1i}}}\right] \quad (3)$$

$$\mathrm{Var}(z_i) \approx \frac{\hat{\sigma}^2_{\hat{\beta}_{1i}}}{\left(\mu_{\hat{z}_i}\right)^4}.$$

We then estimated broad-sense heritability as:

$$H^2_{CT_{max}} = \frac{\mathrm{Var}\left(\mathrm{CT}_{\max_i}\right)}{\mathrm{Var}\left(\mathrm{CT}_{\max_i}\right) + \mathrm{Var}(z_i) + \frac{\hat{\sigma}^2_{\varepsilon}}{n_0}}, \quad (4)$$

$$H^2_{z} = \frac{\mathrm{Var}(\hat{z}_i)}{\mathrm{Var}\left(\mathrm{CT}_{\max_i}\right) + \mathrm{Var}(z_i) + \frac{\hat{\sigma}^2_{\varepsilon}}{n_0}},$$

where

$$n_0 = \frac{1}{a-1}\left(\sum_{i=1}^{a} n_i - \frac{\sum_{i=1}^{a} n_1^2}{\sum_{i=1}^{a} n_i}\right) \quad (5)$$

is the appropriate mean value of the number of flies from each sex and DGRP line used at each stressful temperature to estimate the TDT curves [32, p. 212] The reason we divided the residual variance by n_0 is because we are using line means [33]. In our case $n_0 = 10.2$ for females and $n_0 = 10.8$ for males.

Delete-one-DRGP genotype at a time data resampling was also carried out to estimate the genetic components of variance and their standard errors [34]. A total of 20 pseudovalues for each sex were obtained by dropping, in turn, each DGRP line and calculating:

$$\phi_i = N\hat{\theta}_N - (N-1)\hat{\theta}_{N-1,i}, \quad (6)$$

where ϕ_i is the *i*th pseudovalue, $\hat{\theta}_N$ is the corresponding variance estimate using all $N = 20$ DGRP genotypes, and $\hat{\theta}_{N-1,i}$ is that estimate by dropping the *i*th DGRP genotype alone. The jackknife estimate is the average of ϕ_i , and its standard error is given by

$$\mathrm{SE} = \sqrt{\frac{\sum_{i=1}^{i=N}(\phi_i - \bar{\phi})^2}{N(N-1)}}. \quad (7)$$

Approximate 95% jackknife confidence intervals were obtained as $\bar{\phi} \pm 2\,\mathrm{SE}$. Initially, the analyses for computing variance components and heritability were implemented by MS in MATLAB. To enhance reproducibility, FPL and EJN replicated the analyses and implemented them in R version 4.3.2 [35]. The data used in these analyses were based on a recently reported study [21,36].

(d) Simulated selection on the TDT curves

Appropriate estimates of the additive-genetic G and phenotypic P (co)variance matrices in an outbred *Drosophila* population are needed to explore the evolutionary consequences of selection on CTmax and *z* from the multivariate breeder's equation $\Delta\mu = G\beta = \mathrm{GP}^{-1}s$. Here, the term $\Delta\mu$ is the vector of changes in trait means, β is the vector of selection gradients, and s is the vector of selection differentials [37,38].

The estimates of genetic variance-covariance components and broad-sense heritability in the highly inbred DGRP lines yield only the relative contributions of CTmax and z to the total genetic variance in the TDT curves [see 33]. To our knowledge, there are no estimates of the narrow-sense heritability of TDT curves. Current evidence suggests that upper critical limits estimated with different methodologies is moderately heritable, and it seems reasonable to assume that its narrow-sense heritability is $h^2 \approx 0.25$ [17,39,40]. Based on this information and the relative contribution of CTmax and *z* to the total genetic variance of TDT curves, we quantified the consequences of several simulated selective scenarios on the evolution of thermal tolerance (represented by these two parameters in the TDT curves) in an outbred population. Note that this will be "what-if" scenarios and more accurate estimates of G and P would be needed for a more satisfactory answer.

3. Results

(a) Determination of TDT curves and variance components

We observed substantial variation in thermal death time (TDT) curves across genetic lines for both females and males (Figure 1). At 36°C, the average survival times (± SD) were 150 ± 47 minutes for females and 111 ± 41.6 minutes for males. These durations decreased significantly at 39°C, with females surviving for 12.7 ± 5.13 minutes and males for 14.7 ± 5.6 minutes on average. Notably, this variation in thermal tolerance across genetic lines was consistently observed for both sexes (Figure 1).

Table 1 provides estimates of the variance-covariance components and broad-sense heritability using different methods for estimating parameters in the linear mixed-effects model. These estimates were highly consistent across the various methods of estimation. As indicated by the jackknife 95% confidence intervals, all variance components were significantly different from zero. Furthermore, the genetic covariance between $\beta_0$and β_1 was negative. Broad-sense heritability was around 0.75 for CTmax and around 0.25 for *z*. In other words, CTmax accounts for approximately 75% and *z* accounts for approximately 25% of the total genetic variance in the TDT curves.

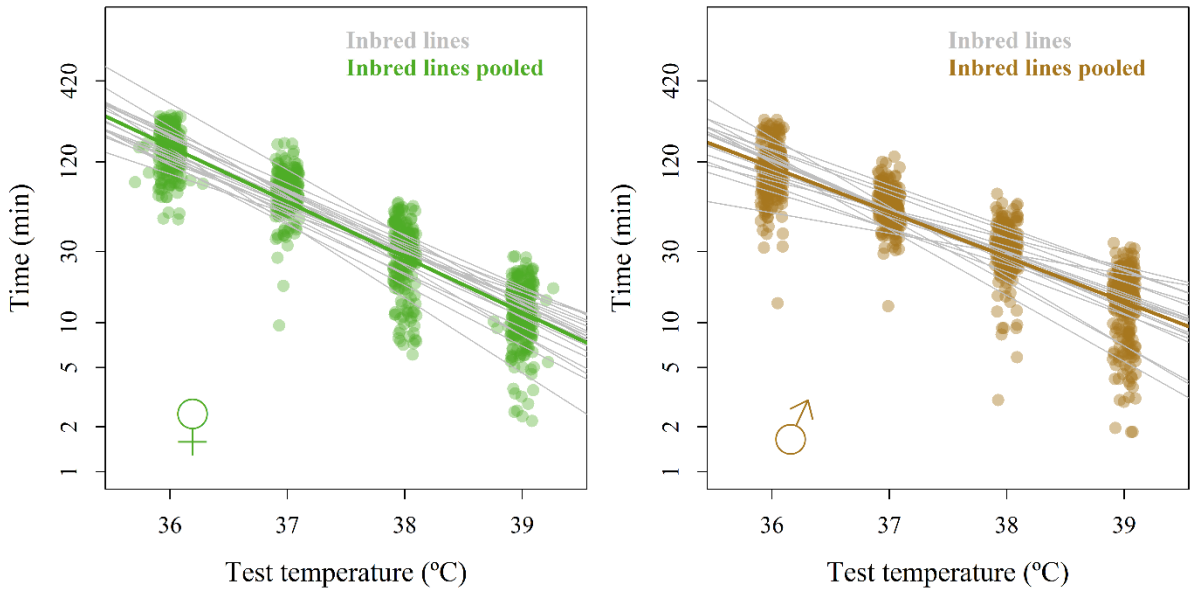

Figure 1. Thermal death time (*y*-axis in $\log_{10}$-scale) curves for females (left) and males (top). Dots represent the individual survival time for females (green, left plot) and males (brown, right plot).

Table 1. Estimation of variance-covariance components and broad-sense heritability using multiple approaches for parameters estimation in the linear mixed-effects model described in equation (2). Estimates were obtained with MATLAB.

Method	Component	Females				Males			
		Estimate	Jackknife	Lower 95% CI	Upper 95% CI	Estimate	Jackknife	Lower 95% CI	Upper 95% CI
ANOVA	$\hat{\sigma}^2_{\hat{\beta}_{0i}}$	4.176376	4.222055	0.818848	7.625262	7.894796	7.885140	1.780019	13.990261
	$\hat{\sigma}^2_{\hat{\beta}_{1i}}$	0.003093	0.003131	0.000591	0.005671	0.005759	0.005753	0.001330	0.010175
	$Cov(\hat{\beta}_0, \hat{\beta}_1)$	-0.113664	-0.114983	-0.207922	-0.022044	-0.213231	-0.212990	-0.377274	-0.048706
	σ^2_ε	0.025323	0.025350	0.017416	0.033283	0.022589	0.022626	0.016258	0.028993
	$\sigma^2_{\overline{CT}_{max}}$	0.594709	0.611843	0.095040	1.128645	2.085709	2.079167	0.604101	3.554233
	$\sigma^2_{\hat{z}}$	0.163722	0.167434	0.039708	0.295159	0.689940	0.680720	0.146407	1.215034
	$H^2_{\overline{CT}_{max}}$	0.781584	0.790793	0.713939	0.867647	0.750866	0.750360	0.699404	0.801316
	$H^2_{\hat{z}}$	0.215169	0.206795	0.131965	0.281624	0.248382	0.249001	0.197763	0.300239
ML	$\hat{\sigma}^2_{\hat{\beta}_{0i}}$	3.627185	3.798623	0.851691	6.745556	7.508898	7.906648	1.943793	13.869503
	$\hat{\sigma}^2_{\hat{\beta}_{1i}}$	0.002667	0.002805	0.000611	0.004998	0.005478	0.005781	0.001472	0.010090
	$Cov(\hat{\beta}_0, \hat{\beta}_1)$	-0.098364	-0.103366	-0.183723	-0.023008	-0.202806	-0.214053	-0.374382	-0.053725
	σ^2_ε	0.025342	0.025379	0.017435	0.033323	0.022591	0.022629	0.016262	0.028995
	$\sigma^2_{\overline{CT}_{max}}$	0.486893	0.444964	-0.009015	0.898944	1.984456	1.900759	0.570539	3.230979
	$\sigma^2_{\hat{z}}$	0.141176	0.149578	0.038018	0.261138	0.656208	0.685757	0.170153	1.201361
	$H^2_{\overline{CT}_{max}}$	0.772182	0.758771	0.663605	0.853937	0.750905	0.730511	0.670472	0.790550
	$H^2_{\hat{z}}$	0.223896	0.238107	0.145710	0.330503	0.248304	0.268794	0.208392	0.329196
REML	$\hat{\sigma}^2_{\hat{\beta}_{0i}}$	3.855075	3.790919	0.688634	6.893203	7.934343	7.906623	1.606537	14.206708
	$\hat{\sigma}^2_{\hat{\beta}_{1i}}$	0.002833	0.002803	0.000489	0.005117	0.005787	0.005781	0.001231	0.010332
	$Cov(\hat{\beta}_0, \hat{\beta}_1)$	-0.104513	-0.103320	-0.188112	-0.018528	-0.214281	-0.214055	-0.383359	-0.044751
	σ^2_ε	0.025341	0.025378	0.017435	0.033321	0.022591	0.022629	0.016262	0.028995
	$\sigma^2_{\overline{CT}_{max}}$	0.514967	0.401291	-0.009975	0.812558	2.096738	1.893919	0.422145	3.365694
	$\sigma^2_{\hat{z}}$	0.149959	0.149561	0.031902	0.267221	0.693300	0.685338	0.140733	1.229943
	$H^2_{\overline{CT}_{max}}$	0.771604	0.736672	0.669950	0.803394	0.750946	0.731923	0.679424	0.784421
	$H^2_{\hat{z}}$	0.224691	0.259674	0.193723	0.325625	0.248305	0.267388	0.214568	0.320208

(b) Simulated selection on the TDT curves

We can employ the raw phenotypic (co)variance matrix of the females from the DGRP lines as a representative of the P matrix in an outbred population, omitting any changes in phenotypic variance caused by inbreeding for the sake of simplicity [41]. Let us now assume the absence of epistasis and use the genetic variation in the DGRP lines for CTmax and z (REML estimates for females in Table 1), together with their relative broad-sense heritability, to figure out what the G matrix would look like in an outbred population. Focusing on the univariate trait CTmax, imagine we obtain a narrow-sense heritability $h^2_{\mathrm{CTmax}} \approx 0.25$, whereas focusing on z we obtain a narrow-sense heritability $h^2_z \approx 0.07$, i.e. about one third the heritability for CTmax. Rescaling the genetic components from the DGRP lines to these values, we could presume the subsequent (co)variance genetic, environmental, and phenotypic matrices for CTmax and z in the hypothetical outbred base population:

$$\mathrm{G} = \begin{bmatrix} 0.1489 & 0.0423 \\ 0.0423 & 0.0133 \end{bmatrix};\ \mathrm{E} = \begin{bmatrix} 0.4466 & 0.2618 \\ 0.2618 & 0.1691 \end{bmatrix};\ \mathrm{P} = \begin{bmatrix} 0.5955 & 0.3041 \\ 0.3041 & 0.1823 \end{bmatrix}$$

The vector of phenotypic means in this base population is $\bar{\mu} = [41.9924 \quad 2.7592]^T$ (*T* stands for transpose), where the first value is for CTmax and the second for *z* (female means from the DGRP lines). We assume that these values are representative of the outbred population, which is strictly true if allelic effects are additive [42].

We simulated three scenarios for increasing thermoresistance (Figure 2): directional selection for CTmax $(s = [1 \quad 0]^T)$, directional selection for both CTmax and *z* $(s = [1 \quad 0.5]^T)$, and directional selection for *z* $(s = [0 \quad 0.5]^T)$. These selection differentials correspond to intensities of selection $i_{\mathrm{CTmax}} = 1.3$ and $i_z = 1.2$. The simulated selection regimes used to illustrate the effects of selection are much stronger than we would expect in nature because directional selection tends to be weak and rarely shifts mean by more than half of a phenotypic standard deviation [43,44]. However, under extreme climatic events, such as heat waves, which are considered to be major triggers of evolution [45], these intensities of selection may not be unrealistic [46].

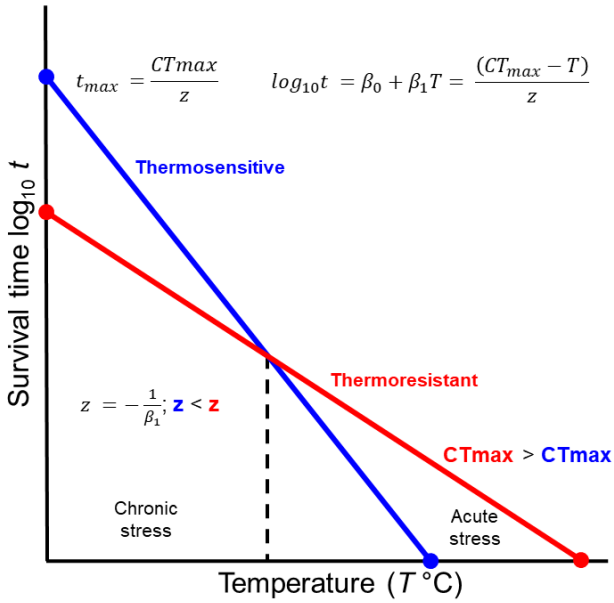

Figure 2. The thermal death time (TDT) curve linearly describes the relationship between test temperature (*T*) and survival time (*t*, $\log_{10}$ scale) under heat stress conditions in *D. melanogaster*. Thermal sensitivity (z) is the reciprocal of the slope (β_1), representing the increase in temperature required to reduce survival time by one order of magnitude (10-fold). CTmax is the intersection at $\log_{10}$ = 0, corresponding to the knockdown or death temperature after 1 minute of exposure. The blue line represents a thermosensitive genotype, which exhibits improved tolerance to acute, intense heat stress but reduced tolerance to chronic, less intense heat. Conversely, the red line depicts a thermoresistant genotype, exhibiting better tolerance to chronic stress but lower tolerance to acute stress.

The simulated scenarios are shown in Figure 3. It is striking that a directional selection gradient always has a different sign than its selection differential, and the evolutionary response can be against the selection differential (Figure 3C). The inference from these hypothetical selection regimes is that directional selection to increase thermal sensitivity *z* seems to hinder evolutionary responses to increasing CTmax. In other words, directional selection to increase CTmax also increases *z* as a correlated response (Figure 3A) and, as expected, drives the population towards a more thermoresistant state (Figure 2). However, directional selection to increase *z* results in a decrease of CTmax as a correlated response, which, in turn, also decreases *z*, and seemingly paradoxically drives the population towards increasing thermosensitivity (Figure 2).

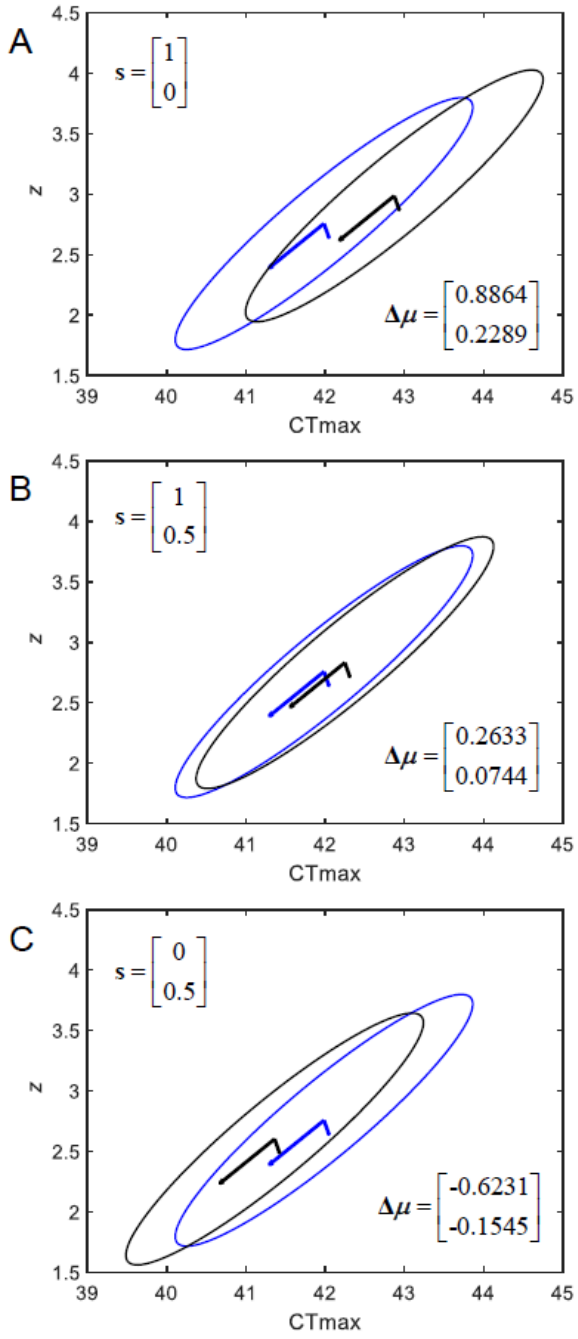

Figure 3. Hypothetical strong directional selection for increased thermoresistance. In blue the 95% confidence ellipses of a simulated population of $N = 10{,}000$ flies from a bivariate normal distribution whose phenotypes for CTmax and *z* are the sum of genetic effects with mean $\bar{\mu} = [41.9924 \quad 2.7592]^T$ and additive-genetic (co)variance G, plus environmental effects with mean 0 and (co)variance E (see text). The arrows centred on the bivariate means represent the directions in which the data vary the most (i.e., the eigenvectors of the covariance matrix of the data). In black are the 95% confidence ellipses after an evolutionary shift in the means (we ignore changes in variance and covariance). Panel A plots directional selection for increasing CTmax; the vector of selection gradients is $\beta = [11.3294 \quad -18.8959]^T$. Panel B plots directional selection for increasing both CTmax and *z*, where $\beta = [1.8814 \quad -0.3958]^T$. Panel C plots directional selection for increasing z, where $\beta = [-9.4480 \quad 18.5002]^T$.

4. Discussion

Heat tolerance has traditionally been examined from a physiological perspective, with a focus on the mechanisms that cause animals to succumb to heat stress, such as oxygen limitation or excessive water loss [see 47 for a review]. In this study, we examine the genetic components of heat tolerance through the lens of thermal death time (TDT) curves. This allows partitioning the relative contribution of CTmax and *z* to the more complex trait "thermotolerance" (Figure 2). Our approach has relied on inbred *Drosophila melanogaster* lines from the DGRP panel, and it would be highly desirable to extend these analyses to outbred populations.

The limited number of previous studies that have assessed the thermal tolerance of DGRP lines focused primarily on measuring critical thermal limits with heating assays [48,49]. These, along with other studies [12,50], suggest that heat tolerance is somewhat evolutionary constrained, an idea often invoked to explain the absence of strong latitudinal clines in heat tolerance, at least in terrestrial ectotherms [13]. Typically, assessments of organisms' vulnerability to global warming usually compare experimentally derived thermal limits using dynamic trials, in which animals are exposed to increasingly higher temperatures [15,51]. During these trials, the intensity and duration of stress increase concurrently. As a result, animals often succumb to heat stress in rapid succession, leading to small variances and small standard deviations in the measurements, making CTmax an attractive endpoint to use in treatment comparisons. However, CTmax is a single point, whereas the trait of interest, namely the ability of an organism to deal with heat stress, is a linear function describing how stress intensity and stress duration impact survival [26]. Thus, ramping trials approach overlooks the cumulative nature of heat injury and the time-dependent effects of thermal tolerance [52–54], potentially underestimating organisms' vulnerability to global warming [55]. We contend that utilizing TDT curves to evaluate both CTmax and *z* parameters, as well as their underlying genetic basis, would provide more accurate predictions. Here, we have developed a methodological approach to estimate the variance components and heritability of the relevant parameters in the TDT curves.

The hypothetical selection scenarios allow us to understand how thermosensitive and thermotolerant strategies (Figure 2) could evolve. They suggest that thermosensitive or thermotolerant strategies are better achieved by directional selection to decrease or increase CTmax. This conclusion holds in more realistic scenarios, where the intensity of selection on CTmax and/or *z* might be relatively weak. We acknowledge that our approach is only a rough estimate of the problem and that several caveats could be raised. For instance, although there is a high positive correlation across species for parameters CTmax and *z* ($r = 0.92$; [26]), the G matrix used to simulate the selection scenarios could overestimate the additive genetic covariance in an outbred *Drosophila* population due to higher linkage disequilibria in the DGRP lines [33]. For the time being, however, we offer the somewhat unexpected results as a cautionary tale about drawing conclusions without considering the multivariate nature of the trait thermal tolerance.

In summary, our findings suggest that the genetic correlation between CTmax and z impose constraints on thermal tolerance strategies. The simulations performed here highlight the importance of considering the multivariate nature of thermal tolerance traits and their genetic correlations when predicting evolutionary responses to climate change. Ultimately,

this can be achieved by utilizing approaches that measure thermal tolerances considering both the duration and intensity of heat stress and its potential for evolution. Adopting such integrative approaches will enable more accurate predictions of how species might respond to increasing temperatures in a rapidly changing planet.

Data accessibility

Data files and code supporting analyses, figures and tables of this study are publicly available on GitHub (https://github.com/felixpleiva/Genetic_variation_TDT). When using the code from this manuscript, please cite it as [56]: Leiva FP, Santos M, Niklitschek EJ, Rezende EL, & Verberk WCEP. (2024). Paper data and code for: Genetic variation of heat tolerance in a model ectotherm: an approach using thermal death time curves. Zenodo. https://doi.org/10.5281/zenodo.12155988.

Authors' contributions

Félix P. Leiva: conceptualization, data curation, formal analysis, funding acquisition, investigation, methodology, project administration, resources, software, validation, visualization, writing – original draft preparation, writing – review and editing; Mauro Santos: conceptualization, formal analysis, methodology, software, writing – original draft preparation, writing – review and editing; Edwin J. Niklitschek: formal analysis, software, validation, writing – review and editing; Enrico L. Rezende: conceptualization, investigation, writing – review and editing; Wilco C.E.P. Verberk: conceptualization, formal analysis, funding acquisition, investigation, methodology, resources, supervision, writing – review and editing. All authors gave final approval for publication.

Funding

This work was supported by the Alexander von Humboldt Foundation; the National Agency for Research and Development (ANID, Chile) [grant number Becas Chile 2018-72190288, PIA/BASAL FB0002]; Ministerio de Ciencia e Innovación (Spain) [grant number PID2021-127107NB-I00]; Generalitat de Catalunya [grant number 2021 SGR 00526]; the Distinguished Guest Scientists Fellowship Programme of the Hungarian Academy of Sciences (https://mta.hu); FONDECYT (Chile) [grant number 1211113]; and The Netherlands Organisation for Scientific Research (grant number VIDI 016.161.321).

Acknowledgements

We thank Cecilia Balboa for kindly assisting with video checking.

References

1. 2019 IPCC, 2018: Global Warming of 1.5°C. An IPCC Special Report on the impacts of global warming of 1.5°C above pre-industrial levels and related global greenhouse gas emission pathways, in the context of strengthening the global response to the threat of climate change, sustainable development, and efforts to eradicate poverty. Cambridge, UK and New York, NY, USA: Cambridge University Press.

2. Huey RB, Stevenson RD. 1979 Integrating thermal physiology and ecology of ectotherms: a discussion of approaches. American Zoologist , 357–366.

3. Rezende EL, Bozinovic F. 2019 Thermal performance across levels of biological organization. Philosophical Transactions of the Royal Society B **374**, 20180549.

4. Pinsky ML, Selden RL, Kitchel ZJ. 2019 Climate-driven shifts in marine species ranges: scaling from organisms to communities. Annual review of marine science **12**, 153–179.

5. Urban MC. 2015 Accelerating extinction risk from climate change. Science **348**, 571–573.

6. Hoffmann AA, Hercus MJ. 2000 Environmental stress as an evolutionary force. BioScience **50**, 217–226.

7. Gunderson AR, Dillon ME, Stillman JH. 2017 Estimating the benefits of plasticity in ectotherm heat tolerance under natural thermal variability. Functional Ecology **31**, 1529–1539.

8. Rudman Seth M., Greenblum Sharon I., Rajpurohit Subhash, Betancourt Nicolas J., Hanna Jinjoo, Tilk Susanne, Yokoyama Tuya, Petrov Dmitri A., Schmidt Paul. 2022 Direct observation of adaptive tracking on ecological time scales in Drosophila. Science **375**, eabj7484. (doi:10.1126/science.abj7484)

9. Huey RB, Kingsolver JG. 1993 Evolution of resistance to high temperature in ectotherms. American Naturalist , S21–S46.

10. Rezende EL, Tejedo M, Santos M. 2011 Estimating the adaptive potential of critical thermal limits: methodological problems and evolutionary implications. Functional Ecology **25**, 111–121.

11. Santos M, Castañeda LE, Rezende EL. 2011 Making sense of heat tolerance estimates in ectotherms: lessons from Drosophila. Functional Ecology **25**, 1169–1180.

12. Hoffmann AA, Chown SL, Clusella-Trullas S. 2013 Upper thermal limits in terrestrial ectotherms: how constrained are they? Functional Ecology **27**, 934–949.

13. Araújo MB, Ferri-Yáñez F, Bozinovic F, Marquet PA, Valladares F, Chown SL. 2013 Heat freezes niche evolution. Ecology Letters **16**, 1206–1219. (doi:https://doi.org/10.1111/ele.12155)

14. Sunday JM, Bates AE, Dulvy NK. 2011 Global analysis of thermal tolerance and latitude in ectotherms. Proceedings of the Royal Society of London B: Biological Sciences **278**, 1823–1830. (doi:https://doi.org/10.1098/rspb.2010.1295)

15. Sunday JM et al. 2019 Thermal tolerance patterns across latitude and elevation. Philosophical Transactions of the Royal Society B: Biological Sciences **374**. (doi:10.1098/rstb.2019.0036)

16. Hutchison VH. 1961 Critical Thermal Maxima in Salamanders. Physiological Zoology **34**, 92–125. (doi:10.1086/physzool.34.2.30152688)

17. Santos M, Castañeda LE, Rezende EL. 2012 Keeping pace with climate change: what is wrong with the evolutionary potential of upper thermal limits? Ecology and Evolution **2**, 2866–2880. (doi:10.1002/ece3.385)

18. Leiva FP, Boerrigter JG, Verberk WCEP. 2023 The role of cell size in shaping responses to oxygen and temperature in fruit flies. Functional Ecology **37**, 1269–1279. (doi:10.1111/1365-2435.14294)

19. Burton T, Einum S. 2020 The old and the large may suffer disproportionately during episodes of high temperature: evidence from a keystone zooplankton species. Conservation Physiology **8**, coaa038.

20. Castañeda LE, Rezende EL, Santos M. 2015 Heat tolerance in Drosophila subobscura along a latitudinal gradient: contrasting patterns between plastic and genetic responses. Evolution **69**, 2721–2734.

21. Leiva FP, Santos M, Rezende EL, Verberk WCEP. 2024 Intraspecific variation of heat tolerance in a model ectotherm: The role of oxygen, cell size and body size. Functional Ecology **38**, 439–448. (doi:10.1111/1365-2435.14485)

22. Truebano M, Fenner P, Tills O, Rundle SD, Rezende EL. 2018 Thermal strategies vary with life history stage. Journal of Experimental Biology **221**, jeb171629.

23. Verberk WCEP, Hoefnagel KN, Peralta-Maraver I, Floury M, Rezende EL. 2023 Long-term forecast of thermal mortality with climate warming in riverine amphipods. Global Change Biology **29**, 5033–5043. (doi:10.1111/gcb.16834)

24. Verspagen N, Leiva FP, Janssen I, Verberk WCEP. 2020 Effects of developmental plasticity on heat tolerance may be mediated by changes in cell size in Drosophila melanogaster. Insect Science **27**, 1244–1256. (doi:10.1111/1744-7917.12742)

25. Bigelow W. 1921 The logarithmic nature of thermal death time curves. The Journal of Infectious Diseases , 528–536.

26. Rezende EL, Castañeda LE, Santos M. 2014 Tolerance landscapes in thermal ecology. Functional Ecology **28**, 799–809.

27. Wang S, Tang J, Hansen JD. 2007 Experimental and simulation methods of insect thermal death kinetics. In Heat Treatments for Postharvest Pest Control: Theory and Practice (eds J Tang, EJ Mitcham, S Wang, S Lurie), pp. 105–132. Oxon, UK: CABI Publishing.

28. Leiva FP, Santos M, Rezende EL, Verberk WCEP. 2023 Intraspecific variation on heat tolerance in a model ectotherm: the role of oxygen, cell size and body size. Functional Ecology (doi:10.1111/1365-2435.14485)

29. Mackay TF et al. 2012 The Drosophila melanogaster genetic reference panel. Nature **482**, 173–178.

30. 2007 STATISTICA (data analysis software system).

31. Wolter KM. 2007 Introduction to Variance Estimation. New York, NY: Springer New York. (doi:10.1007/978-0-387-35099-8)

32. Sokal RR, Rohlf FJ. 1995 Biometry. New York.

33. Mackay TFC, Huang W. 2018 Charting the genotype–phenotype map: lessons from the Drosophila melanogaster Genetic Reference Panel. WIREs Developmental Biology **7**, e289. (doi:10.1002/wdev.289)

34. Knapp SJ, Bridges-Jr WC, Yang M-H. 1989 Nonparametric confidence interval estimators for heritability and expected selection response. Genetics **121**, 891–898.

35. R Development Core Team. 2023 R: A language and environment for statistical computing. R Foundation for Statistical Computing, Vienna, Austria.

36. Leiva FP, Santos M, Rezende EL, Verberk WCEP. 2021 Paper data and code of manuscript: Intraspecific variation on heat tolerance in a model ectotherm: effects of body mass, cell size, oxygen and sex. Zenodo. (doi:https://doi.org/10.5281/zenodo.5120028)

37. Lande R. 1979 Quantitative genetic analysis of multivariate evolution, applied to brain: body size allometry. Evolution **33**, 402–416.

38. Lande R, Arnold SJ. 1983 The measurement of selection on correlated characters. Evolution **37**, 1210–1226.

39. Diamond SE. 2017 Evolutionary potential of upper thermal tolerance: biogeographic patterns and expectations under climate change. Annals of the New York Academy of Sciences **1389**, 5–19. (doi:10.1111/nyas.13223)

40. Logan ML, Cox CL. 2020 Genetic constraints, transcriptome plasticity, and the evolutionary response to climate change. Frontiers in Genetics **11**, 538226.

41. Fowler K, Whitlock MC. 1999 The distribution of phenotypic variance with inbreeding. Evolution **53**, 1143–1156. (doi:10.2307/2640818)

42. Falconer DS, Mackay TFC. 1996 Introduction to quantitative genetics. 4th edn. Pearson Education India.

43. Endler JA. 1986 Natural selection in the wild. Princeton University Press.

44. Kingsolver JG, Hoekstra HE, Hoekstra JM, Berrigan D, Vignieri SN, Hill CE, Hoang A, Gibert P, Beerli P. 2001 The Strength of Phenotypic Selection in Natural Populations. The American Naturalist **157**, 245–261. (doi:10.1086/319193)

45. Grant PR, Grant BR, Huey RB, Johnson MTJ, Knoll AH, Schmitt J. 2017 Evolution caused by extreme events. Phil. Trans. R. Soc. B **372**, 20160146. (doi:10.1098/rstb.2016.0146)

46. Rodríguez-Trelles F, Tarrío R, Santos M. 2013 Genome-wide evolutionary response to a heat wave in Drosophila. Biol. Lett. **9**, 20130228. (doi:10.1098/rsbl.2013.0228)

47. MacMillan HA. 2019 Dissecting cause from consequence: a systematic approach to thermal limits. Journal of Experimental Biology **222**, jeb191593.

48. Lecheta MC et al. 2020 Integrating GWAS and Transcriptomics to Identify the Molecular Underpinnings of Thermal Stress Responses in Drosophila melanogaster. Frontiers in Genetics **11**, 658. (doi:10.3389/fgene.2020.00658)

49. Rolandi C, Lighton JRB, de la Vega GJ, Schilman PE, Mensch J. 2018 Genetic variation for tolerance to high temperatures in a population of Drosophila melanogaster. Ecology and Evolution **8**, 10374–10383. (doi:10.1002/ece3.4409)

50. Kellermann V, Overgaard J, Hoffmann AA, Fløjgaard C, Svenning J-C, Loeschcke V. 2012 Upper thermal limits of Drosophila are linked to species distributions and strongly constrained phylogenetically. Proceedings of the National Academy of Sciences **109**, 16228–16233.

51. Leiva FP, Calosi P, Verberk WCEP. 2019 Scaling of thermal tolerance with body mass and genome size in ectotherms: A comparison between water-and air-breathers. Philosophical Transactions of the Royal Society B: Biological Sciences **374**, 20190035. (doi:10.1098/rstb.2019.0035)

52. Rezende EL, Bozinovic F, Szilágyi A, Santos M. 2020 Predicting temperature mortality and selection in natural Drosophila populations. Science **369**, 1242–1245.

53. Jørgensen LB, Malte H, Overgaard J. 2019 How to assess Drosophila heat tolerance: Unifying static and dynamic tolerance assays to predict heat distribution limits. Functional Ecology **33**, 629–642. (doi:10.1111/1365-2435.132)

54. Jørgensen LB, Malte H, Ørsted M, Klahn NA, Overgaard J. 2021 A unifying model to estimate thermal tolerance limits in ectotherms across static, dynamic and fluctuating exposures to thermal stress. Scientific reports **11**, 1–14.

55. Huey RB, Kearney MR. 2020 Dynamics of death by heat. Science **369**, 1163–1163. (doi:10.1126/science.abe0320)

56. Leiva FP, Santos M, Niklitschek EJ, Rezende EL, Verberk WCEP. 2024 Paper data and code for: Genetic variation of heat tolerance in a model ectotherm: an approach using thermal death time curves. Zenodo. (doi:https://doi.org/10.5281/zenodo.12155988)